ELSEVIER

Computer Networks and ISDN Systems 29 (1998) 2103–2117

COMPUTER NETWORKS and ISDN SYSTEMS

Evaluation of ABR traffic management under various system time scales [1]

Tamer Dağ, Ioannis Stavrakakis *

Electrical and Computer Engineering Department, 409 Dana Research Building, 360 Huntington Avenue, Northeastern University, Boston, MA 02115, USA

Abstract

In this paper, the effects of various time scales on the management of ABR (Available Bit Rate) traffic using feedback based control is studied. Since delay tolerable, the ABR applications can be allocated the remaining resources after CBR (Constant Bit Rate) and VBR (Variable Bit Rate) applications have been accommodated. To avoid excessive losses the transmission rate of the ABR applications should be modulated by the amount of remaining resources. That is, the ABR rate should be controlled through a feedback based rate control mechanism. In this paper, a network link shared by remote ABR and VBR applications is considered and the impact of various system time scales on the effectiveness of the feedback based flow control scheme is investigated by formulating and studying a tractable analytical model. These time scales are expressed in terms of the network transmission speed, the minimum tolerable ABR rate and the rate of change of the VBR source rate. While the negative impact of a decreased network time scale on the effectiveness of this control scheme is well established, the impact of the ABR and VBR time scales has not been investigated in the past. It turns out that for a given network time scale, the induced cell losses can be significantly reduced for increased ABR and/or VBR time scales and thus, the latter time scales should be taken into consideration while evaluating the effectiveness of an adaptive feedback based flow control mechanism. This study also suggests that higher efficiency can be achieved by enforcing large ABR time scales, leading to the introduction of a new class of transmission policies. © 1998 Elsevier Science B.V.

Keywords: Time scale; ABR; VBR; Flow control

1. Introduction

Asynchronous Transfer Mode (ATM) has been chosen as the CCITT standard for the switching and multiplexing technique of the Broadband-Integrated Services Digital Networks (B-ISDN) currently under development. ATM networks are expected to support applications with diverse traffic characteristics and Quality of Service (QoS) requirements such as data transfer, video, voice, multi-media conference and real time control.

ATM is primarily a connection oriented protocol. Virtual circuits are set and the route is decided at connection set up. Connection oriented services have typically long sustained sessions and cells are transmitted

* Corresponding author. E-mail: ioannis@hilbert.cdsp.neu.edu.

[1] This research is supported by the National Science Foundation under Grant NCR-9628116.

PII S0169-7552(97)00119-0

and delivered in order. Therefore, it appears like a dedicated link where all cells associated with a service follow the same path. Statistical multiplexing is possible by on-demand transmitting cells from different sources over the same line and storing them temporarily in shared buffers within the network.

The ATM Forum [1] has defined four different service classes. Constant Bit Rate (CBR), Variable Bit Rate (VBR), Available Bit Rate (ABR) and Unspecified Bit Rate (UBR). These classes cover a broad spectrum of diverse applications. Non-real time VBR, ABR and UBR service classes are intended for non-real time applications, while CBR and real time VBR are intended for real time applications.

The ABR service class that is intended for non-real time applications can tolerate delay. This service class simply uses the remaining capacity left from VBR and CBR services and thus it is a best effort service class. The goal of this service class is to use the unused network bandwidth as efficiently as possible. For the ABR service class the only negotiated QoS parameter is the Cell Loss Ratio (CLR) and is not necessarily quantified. Peak Cell Rate (PCR), Cell Delay Variation Tolerance (CDVT) and Minimum Cell Rate (MCR) are the traffic parameters.

The ABR service class is different from the other service classes in many ways [2]. The available bandwidth will be shared by the ABR connections and will change dynamically due to the fluctuations in the VBR and CBR traffics and therefore it may reduce to the MCR. Since VBR and CBR traffic rates will fluctuate in time, the ABR sources should adjust their rates to these fluctuations in order to utilize the entire remaining capacity or avoid cell losses.

These characteristics point to the necessity of controlling the flow of the ABR traffic sources. Two major flow control mechanisms for the ABR service have been considered: The rate based flow control [3–5] and the credit based flow control [6–8]. Since both of these flow control schemes have some advantages and disadvantages, there were also studies on the integration of both schemes [9].

The credit based flow control is implemented link by link and per virtual circuit (VC). Before transmitting any cells over the link, the sender associated with the VC link needs to receive credits for the VC from the receiver. The credit indicates the amount of free buffer space available for the sender. The sender can not transmit more cells than its credit. If it uses all its credits, it must wait for other credits. Because of this reason, credit based flow control ensures zero cell loss.

In rate based flow control, the sender is notified about congestion in the network with a feedback generated from the receiver or from the congested node. When the sender receives such a feedback, it adjusts its rate according to the feedback control policy in effect. Although the credit based flow control can handle both smooth and bursty traffic (while the rate based flow control may not be very effective for bursty traffic), it introduces an excessive amount of overhead and it would be very expensive for a wide area network. For such reasons, the more flexible rate based flow control has been adopted by the ATM Forum.

Several different traffic control policies have been proposed for the rate based flow control such as the Explicit Forward Congestion Indication (EFCI) [10], Backward Explicit Congestion Notification (BECN) [11], Proportional Rate Control Algorithm (PRCA) [12], Explicit Rate Feedback (ERF) [13] and Enhanced Proportional Rate Control Algorithm (EPRCA) [14].

Under the feedback based flow control policy used in this paper, a feedback carrying information about the available bandwidth is transmitted to the ABR source when the bandwidth availability for the ABR source changes. But, if the propagation delay between the ABR source and the network access node is non-zero, then the ABR source will transmit at a rate based on the most recent level of available bandwidth until it receives the feedback. Consequently, the effectiveness of the rate based flow control schemes will decrease under increased propagation delays.

For example, if the propagation delay between the ABR source and the network access node is T_d and the available bandwidth changes at time t, the ABR source will learn about the change in bandwidth availability at time $t + T_d$. The adjusted rate from the ABR source will reach the network access node at time $t + 2T_d$, assuming that the backward and forward propagation delays are equal. This can be clearly observed in Fig. 1 where the ABR rate, VBR/CBR rate and the total rate at the network access node are shown with respect to

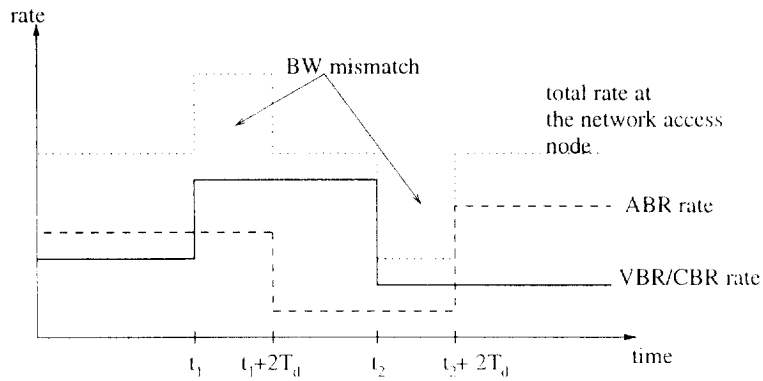

Fig. 1. An example of bandwidth mismatch.

time. The ABR application uses the remaining bandwidth left from VBR/CBR applications and whenever the VBR/CBR applications change their rates, a bandwidth mismatch occurs for a duration equal to the roundtrip propagation delay of $2T_d$.

When a decrease in the remaining bandwidth occurs, the link capacity is exceeded for a duration of $2T_d$ and overutilization occurs. During an overutilization period, the number of cells in transit becomes excessive and cell losses occur. When an increase in the remaining bandwidth occurs, underutilization occurs for a duration of $2T_d$.

While the effects of increased propagation delay on the flow control schemes has been studied in the past [15–18], almost no effort has been focused on the study of the impact of other system parameters. In this paper, the impact of these system parameters (network, ABR and VBR time scales) on the feedback based flow control is investigated.

The network time scale is defined to be the transmission time of a cell (slot). As the network time scale decreases, the propagation delay (measured in slots) increases. Thus, the decreased network time scale has a similar impact on a feedback based flow control schemes as the increased propagation delay.

The frequency of change of the bandwidth availability would also impact significantly on the effectiveness of a feedback based flow control scheme. If over a given time interval the number of VBR/CBR source rate changes increases, then the number of initiated bandwidth mismatch cycles will typically increase as well. Since increased number of bandwidth mismatch cycles will increase the number of overutilization periods, more cell losses will be induced and the effectiveness of the feedback based flow control schemes will be reduced. The VBR time scale can be defined as the inverse of the frequency of the VBR source rate changes or the average time over which the VBR application maintains a constant rate. The VBR time scale will be employed in order to capture the impact of the frequency of bandwidth mismatch cycles on the effectiveness of feedback based flow control schemes.

In addition to the network and VBR time scales, the cell transmission patterns of the ABR sources may also impact on the effectiveness of feedback based flow control schemes. It can be observed that between two ABR applications of the same rate, the one which transmits blocks of multiple cells every one of longer periods may utilize the resources better than the one which transmits one cell every one of shorter periods. The ABR time scale is defined here as the length of these periods and will describe the various transmission patterns considered in this paper.

The remainder of the paper is organized as follows. In Section 2, the system considered to evaluate the impact of time scales is described. In Section 3, a suitable Markov Chain for the system is formulated. Some numerical results are presented in Section 4. The paper concludes with the conclusions made in Section 5.

2. Description of the system

Consider a transmission link shared by Variable Bit Rate (VBR) and Available Bit Rate (ABR) applications where the VBR sources are provided prioritized access to the resources and ABR sources are allocated the remaining resources. In order to simplify the analysis and facilitate the understanding of the impact of the various time scales, a system with one VBR source and one ABR source is considered and each of these sources will deliver at most one cell per slot according to the rate in effect.

The ABR traffic source is assumed to be away from the network access node and thus the propagation delay between the ABR source and the network access node is non-negligible. The ABR source is controllable. Its transmission rates are calculated by the network access node by taking into consideration the current VBR transmission rates. The ABR source rates should be calculated appropriately in order not to cause instability. Therefore, the total ABR and VBR source rates at any time instant should not exceed the link capacity.

The network access node is supposed to be able to detect a change in the VBR source rate. This may be possible through an explicit indication that the VBR source carries by certain cells or an estimation mechanism implemented at the network access node. When a rate change for the VBR source occurs, the network access node detects it and calculates the appropriate transmission rate for the ABR source. Then, this information is fed back to the ABR source.

Because of the non-zero propagation delay T_d between the ABR traffic source and the network access node, bandwidth mismatch will occur every time VBR traffic rate changes occur. As described earlier, a change in the VBR rate at time t will be detected by the ABR source at time $t + T_d$ and the adjusted ABR rate will reach the network access node at time $t + 2T_d$. During the above round-trip propagation delay $2T_d$, the network may either be underutilized or overutilized where overutilization is the main reason causing cell losses.

The network access node is assumed to have a finite buffer of capacity C for the temporary storage of the ABR and VBR cells.

A queuing model of the network access node is shown in Fig. 2. The service policy is assumed to be work conserving and VBR cell arrivals are provided head of line (*HoL*) priority as indicated above. ABR cells are served according to the first come first served (FCFS) policy. Cell departures are assumed to occur before cell arrivals occurring over the same slot.

2.1. The ABR traffic source

The maximum allowable ABR source rate is determined by the current VBR source rate. If the latter is equal to r_v, then the maximum allowable ABR source rate will be $1 - r_v - \epsilon$, where ϵ is a small positive number determined by the desirable load at the network access node.

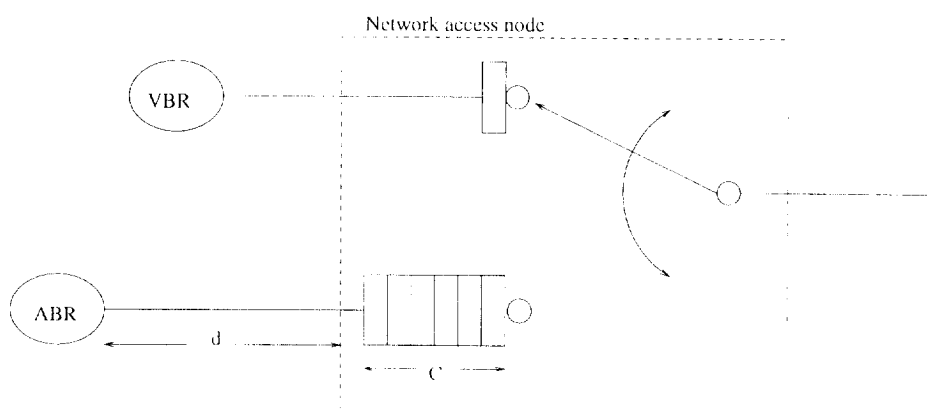

Fig. 2. The queuing model of the network access node.

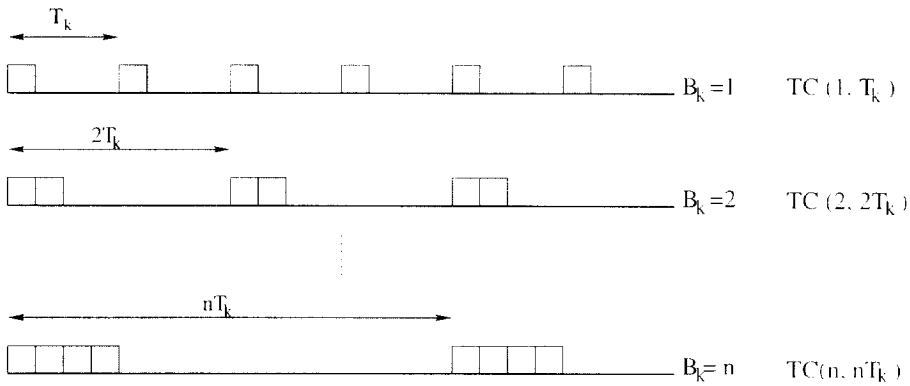

Fig. 3. The ABR traffic subframes.

To achieve a rate close to its maximum allowable value, the ABR source can transmit one cell per T_k slots where $T_k = \lceil 1/(1 - r_v - \epsilon) \rceil$ and $\lceil 0 \rceil$ denotes the smallest integer larger than 0. In this paper, T_k will be referred to as the *fundamental ABR subframe*. The same rate can also be achieved, if the ABR source transmits a block of B_k cells per subframe of length $B_k T_k$, that is, if the ABR source employs a B_k-order subframe, where $B_k \in N$.

Thus, if $B_k = 1$, the ABR source will employ the fundamental subframe T_k to transmit at a rate equal to $1/T_k$. If $B_k > 1$, the ABR source will employ a B_k-order subframe to transmit at the same rate equal to $1/T_k$. Fig. 3 shows examples of ABR cell transmission employing the fundamental and higher-order subframes.

Let $TC(B_k, B_k T_k)$ denote a transmission control policy according to which the ABR source transmits a batch with size B_k at the beginning of a subframe of length $B_k T_k$. Let $\overline{TC}(T_k) = \{TC(B_k, B_k T_k), B_k \geq 1\}$ denote the class of all $TC(B_k, B_k T_k)$ policies which implement the same transmission rate of $1/T_k$. This class of policies is characterized by the fundamental subframe of length T_k.

Let t_k denote the beginning time instant of the kth subframe. At t_k, a fundamental subframe T_k (and the ABR rate) will be determined based on the current VBR rate. Any policy in $\overline{TC}(T_k)$ can be selected for the implementation of the ABR source rate of $1/T_k$. As long as the VBR rate remains constant, the same policy will be employed. That is, if $T_{k+1} = T_k$ then $B_{k+1} = B_k$ and $TC(B_k, T_k) \equiv TC(B_{k+1}, T_{k+1})$. However, if a VBR source rate change occurs, then the network access node calculates the new ABR fundamental subframe T_{k+1} and any policy in $\overline{TC}(T_{k+1})$ can be selected.

The ABR time scale is defined as the length of the B_k-order subframe used to transmit ABR cells. The impact of the ABR time scale on the effectiveness of a feedback based flow control scheme is investigated in this paper.

2.2. The VBR traffic source

Although the activity level of the VBR traffic source is not controllable and can change in principle at any slot, it will be assumed that such changes occur only at subframe boundaries for analysis tractability. Therefore, for the VBR source, time is considered to be subframed and VBR source rate changes can occur anywhere in this subframed time.

Let $\{S_k\}_{k \geq 1}$ be a 2-state underlying Markov chain with state space $S = \{0,1\}$. $\{S_k\}_{k \geq 1}$ will be used to describe the VBR source activity level. $\{S_k\}_{k \geq 1}$ is embedded at subframe boundaries $\{t_k\}_{k \geq 1}$ of length $B_k T_k$, where T_k is determined by the perceived remaining capacity as indicated in the previous subsection.

Let $r_v(s_k)$ denote the rate of the VBR source at the kth subframe, $s_k \in S$. Without loss of generality, it is assumed that $r_v(1) > r_v(0)$. The VBR cell arrival process is modeled as a Markov Modulated Bernoulli process.

The probability of transmitting 1(0) cell in a slot of the kth subframe is $r_i(s_k)(1 - r_i(s_k))$. Therefore, the number of VBR cell arrivals during a slot of the kth subframe, $A(s_k)$, is given by

$$A(s_k) = \begin{cases} 1 & \text{with probability } r_i(s_k), \\ 0 & \text{with probability } 1 - r_i(s_k). \end{cases}$$

Let $p_s(s_k)$ denote the probability that S_k changes at the end of the kth subframe at the beginning of which it was in state s_k. $p_s(s_k)$ will reflect the average time over which VBR applications maintain a constant rate (or VBR time scale). If $p_s(0) = p_s(1) = p_s$, then the VBR time scale will be equal to $1/p_s$; otherwise, two time scales may be defined. It is expected that the increased VBR time scale will increase the effectiveness of the feedback based flow control schemes.

3. Analysis of the system

In this section a proper Markov Chain describing the evolution of the system is described by taking into consideration the properties of the ABR and VBR sources described earlier. Since the VBR traffic is provided prioritized service and the maximum number of VBR cell arrivals per slot is 1, no VBR cell losses will occur. For this reason, the analysis will focus on the evaluation of ABR cell losses and the impact of the time scales considered in this paper will be evaluated based on the ABR cell loss probability.

Let $\{S_k, Q_k\}_{k \geq 1}$ be a 2-dimensional process embedded on $\{t_k\}_{k \geq 1}$, where Q_k is a random variable describing the buffer occupancy at t_k, $0 \leq Q_k \leq C$. By definition, S_k determines completely the VBR arrival process.

If the propagation delay T_d is negligible, then S_k determines the ABR cell arrival process as well, because the ABR source will respond to the VBR source rate changes immediately. If the propagation delay is non-negligible – as it is considered to be the case in this paper – the *fundamental ABR subframe* length can be calculated from $T_k = \lceil 1/(1 - r_i(s'_k) - \epsilon) \rceil$ where s'_k is the VBR state $2T_d$ time units earlier. As a consequence, the current state S_k does not determine the arrival process and thus $\{S_k, Q_k\}_{k \geq 1}$ is not a Markov chain.

Although a Markov chain can be constructed to describe the evolution of the system under fixed and non-zero roundtrip propagation delays, a simplifying assumption is made by assuming that the roundtrip propagation delay is random and geometrically distributed with mean $1/p_f$, measured in terms of subframes. Given that a VBR source rate change has occurred, a feedback indicating the VBR source rate change will arrive at the ABR source by the next subframe boundary with probability p_f. Note that, p_f is adjusted based on the current subframe length so that the mean propagation delay under both subframe schemes are equal.

In order to determine the arrival process to the node over the kth subframe, the network access node needs to know the current VBR source rate ($r_i(s_k)$) and whether the current ABR rate is based on the most recent feedback sent by the node or not (that is, whether the feedback's impact is not pending or pending, respectively). Therefore, another random variable is introduced describing the status of the impact of the feedback at t_k.

Let J_k be an indicator function which assumes the value of 1, if the impact of a feedback carrying a VBR source rate change is pending at t_k; that is, if the ABR rate arriving at the node is not adjusted yet. Otherwise, J_k is equal to 0. Then the ABR traffic rate will be completely determined by (S_k, J_k) and it is equal to $1 - r_i(s_k \oplus j_k) - \epsilon$ where $\oplus$ denotes the modulo 2 addition.

Although it is possible that at any time, the impact of more than one feedbacks can be pending, at most one pending feedback will be considered in order to simplify the analysis. This approximation holds true if $\max_{s_k}\{p_s(s_k)\} < p_f$; that is, if the VBR source time scale is much larger than the propagation delay.

Under the above assumptions, it is easy to establish that the stochastic process $\{S_k, J_k, Q_k\}$ embedded at subframe boundaries is a Markov chain with state space $\{(s_k, j_k, q_k): 0 \leq s_k \leq 1, 0 \leq j_k \leq 1, 0 \leq q_k \leq C\}$.

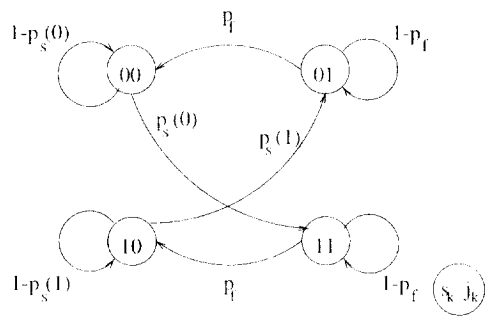

Fig. 4. The state diagram of the $\{S_k, J_k\}$ process.

Let $P(s_k j_k q_k; s_{k+1} j_{k+1} q_{k+1})$ be the probability that the Markov chain $\{S_k, J_k, Q_k\}$ moves from state $(s_k j_k q_k)$ at time t_k, to state $(s_{k+1} j_{k+1} q_{k+1})$ at time t_{k+1}. From the description of the system model, it can be understood that $(s_{k+1} j_{k+1})$ is independent from the queue occupancy q_k and thus $P(s_k j_k q_k; s_{k+1} j_{k+1} q_{k+1})$ can be expressed as follows:

$$P(s_k j_k q_k; s_{k+1} j_{k+1} q_{k+1}) = P(s_k j_k; s_{k+1} j_{k+1}) P(q_{k+1}/s_k j_k q_k).$$

The probabilities on the right side of the above equation can be calculated separately as shown below. Note that $P(s_k j_k; s_{k+1} j_{k+1})$ is the probability of passing from state $(s_k j_k)$ to state $(s_{k+1} j_{k+1})$ and $P(q_{k+1}/s_k j_k q_k)$ is the probability that the queue occupancy at the beginning of the next subframe is q_{k+1}, given the current subframe state $(s_k j_k q_k)$.

The state diagram for the $\{S_k, J_k\}$ process is shown in Fig. 4. Notice that not all state transitions are possible because of the constraint on j_k and the requirement of generating a feedback only when the VBR rate changes. Let $(s_k j_k) \rightarrow (s_{k+1} j_{k+1})$ denote a state transition from $(s_k j_k)$ to $(s_{k+1} j_{k+1})$. For example, a $(00) \rightarrow (10)$

$(s_k j_k)$	$(s_{k+1} j_{k+1})$	$P(s_k j_k, s_{k+1} j_{k+1})$
00	00	$1 - p_s(0)$
00	01	0
00	10	0
00	11	$p_s(0)$
01	00	p_f
01	01	$1 - p_f$
01	10	0
01	11	0
10	00	0
10	01	$p_s(1)$
10	10	$1 - p_s(1)$
10	11	0
11	00	0
11	01	0
11	10	p_f
11	11	$1 - p_f$

transition is impossible, because a pending feedback has to be generated when a VBR rate change occurs. This transition may be possible only if the propagation delay is zero. Similarly, a transition from (11) → (01) can occur with a very low probability which is assumed to be equal to 0. This result comes from the assumption that the VBR source time scale is much larger than the propagation delay.

Let $q_{k,i}$ denote the queue occupancy at the end of the ith slot of the kth subframe and $P_A(q_{k,i+1}/s_k j_k q_{k,i})$ and $P_B(q_{k,i+1}/s_k j_k q_{k,i})$ denote the one slot transition probabilities from $q_{k,i}$ to $q_{k,i+1}$ over the first B_k slots of the kth subframe (where both ABR and VBR cell arrivals are possible) and the remaining $B_k T_k - B_k$ slots (where only VBR cell arrivals are possible); respectively. These probabilities are equal to

$$P_A(q_{k,i+1}/s_k j_k q_{k,i}) = \begin{cases} P\{A(s_k) = q_{k,i+1} - 1\}, & q_{k,i} = 0, 0 \le q_{k,i+1} \le C-1, \\ P\{A(s_k) = q_{k,i+1} - q_{k,i}\}, & 1 \le q_{k,i} \le C, 0 \le q_{k,i+1} \le C-1, \\ \sum_{m=0}^{1+C+q_{k,i}} P\{A(s_k) = C - q_{k,i} + m\}, & 0 \le q_{k,i} \le C, 0 \le q_{k,i+1} \le C. \end{cases}$$

Similarly,

$$P_B(q_{k,i+1}/s_k j_k q_{k,i}) = \begin{cases} P\{A(s_k) = q_{k,i+1}\}, & q_{k,i} = 0, 0 \le q_{k,i+1} \le C, \\ P\{A(s_k) = q_{k,i+1} - q_{k,i} + 1\}, & 1 \le q_{k,i} \le C, 0 \le q_{k,i+1} \le C. \end{cases}$$

Combining these two equations $P(q_{k+1}/s_k j_k q_k)$ can be expressed as follows:

$$P(q_{k+1}/s_k j_k q_k) = \sum_{q_{k,B_k}=0}^{C} P_A(q_{k,B_k}/s_k j_k q_k) P_B(q_{k+1}/s_k j_k q_{k,B_k}).$$

The B_k slot transition probability $P_A(q_{k,B_k}/s_k j_k q_k)$ and $B_k T_k - B_k$ slot transition probability $P_B(q_{k+1}/s_k j_k q_{k,B_k})$ can be calculated iteratively using the 1 slot transition probabilities.

After the calculation of the transition probabilities $P(s_k j_k q_k; s_{k+1} j_{k+1} q_{k+1})$, the steady state probability distribution $\Pi(s_k, j_k, q_k)$ can be derived using the following matrix equations:

$$\Pi = \Pi P,$$
$$\sum_i \Pi_i = 1.$$

where P is the state transition matrix and each of its elements show the transition probabilities $P(s_k j_k q_k; s_{k+1} j_{k+1} q_{k+1})$.

In order to study the impact of network and source time scales, the ABR cell loss probability will be evaluated. The ABR cell loss probability can be calculated using the average number of cells arrived at a subframe in which $\{S_k, J_k, Q_k\}_{k \ge 1}$ is in state $(s_k j_k q_k)$ and taking the expectation over all possible states. Therefore, the ABR cell loss probability denoted by LP is given as

$$LP = E\left\{ \frac{\text{Average number of cells lost in state } (s_k j_k q_k)}{\text{Average number of cells arrived in state } (s_k j_k q_k)} \right\}.$$

Let $\bar{L}(s_k, j_k, q_k)$ and $\bar{M}(s_k, j_k, q_k)$ denote the average number of cells lost and arrived over the subframe at the beginning of which the process $\{S_k, J_k, Q_k\}_{k \ge 1}$ is in state $(s_k j_k q_k)$, respectively. Then,

$$LP = E\left\{ \frac{\bar{L}(s_k, j_k, q_k)}{\bar{M}(s_k, j_k, q_k)} \right\}.$$

In order to calculate $\bar{L}(s_k, j_k, q_k)$ and $\bar{M}(s_k, j_k, q_k)$, $I(s_k, j_k, q_k; i)$ and $R(s_k, j_k; i)$ can be introduced. Let $I(s_k, j_k, q_k; i)$ ($R(s_k, j_k, q_k; i)$) denote the number of cells lost (arrived) at the ith slot of the kth subframe in state $(s_k j_k q_k)$; $1 \le i \le B_k T_k$. Clearly, $R(s_k, j_k, q_k; i)$ does not depend on the queue occupancy and is a function of s_k, j_k and i, since $T_k = f(s_k, j_k)$. Therefore,

$$R(s_k j_k; i) = \begin{cases} A(s_k) & \text{if } i > B_k, \\ A(s_k) + 1 & \text{if } i \le B_k. \end{cases}$$

The number of lost cells in a slot can be found by considering the number of arrivals in that slot, the buffer occupancy in the previous slot and the buffer capacity C. Therefore,

$$I(s_k j_k, q_k; i) = \begin{cases} m & \text{if } R(s_k j_k; i) = C + 1 - q_{k,i-1} + m, \\ 0 & \text{otherwise.} \end{cases}$$

Clearly, the number of cell arrivals over the subframe starting with system Markov Process $\{S_k, J_k, Q_k\}_{k>1}$ in state $(s_k j_k q_k)$ is equal to the summation of $R(s_k, j_k; i)$ for all slots of the subframe. Thus,

$$\begin{aligned} M(s_k, j_k, q_k) &= \sum_{i=1}^{B_k T_k} R(s_k, j_k, q_k) \\ &= \sum_{i=1}^{B_k} (A(s_k) + 1) + \sum_{i=B_k+1}^{B_k T_k} A(s_k) \\ &= B_k + B_k T_k A(s_k). \end{aligned}$$

Taking the expectation of both sides,

$$\bar{M}(s_k, j_k, q_k) = E\{B_k + B_k T_k A(s_k)\} = B_k + B_k T_k r_{j_k}(s_k).$$

The total number of cells lost over the entire subframe is equal to the summation of $I(s_k, j_k, q_k; i)$ for all slots of the subframe:

$$L(s_k, j_k, q_k) = \sum_{i=1}^{B_k T_k} I(s_k, j_k, q_k; i).$$

Taking the expectation of both sides,

$$\bar{L}(s_k, j_k, q_k) = \sum_{i=1}^{B_k T_k} E\{I(s_k, j_k, q_k; i)\}.$$

The above equation can be divided into two terms, the first term corresponding to the first part of the subframe (when both ABR and VBR cell arrivals are possible) and the second term corresponding to the second part of the subframe (when only VBR cell arrivals are possible). Thus,

$$\bar{L}(s_k, j_k, q_k) = \sum_{i=1}^{B_k} E\{I(s_k, j_k, q_k; i)\} + \sum_{i=B_k+1}^{B_k T_k} E\{I(s_k, j_k, q_k; i)\}.$$

By employing the definitions for $I(s_k, j_k, q_k; i)$ and $R(s_k, j_k; i)$ the following expression is obtained:

$$\begin{aligned} \bar{L}(s_k, j_k, q_k) = &\sum_{i=1}^{B_k} \sum_{m} mP\{A(s_k) = C - q_{k,i-1} + m / s_k j_k q_k\} \\ &+ \sum_{i=B_k+1}^{B_k T_k} \sum_{m} mP\{A(s_k) = C + 1 - q_{k,i-1} + m / s_k j_k q_k\}. \end{aligned}$$

Since there are at most one arrivals per slot after the first B_k slots of each subframe, cell losses may occur only in the first B_k slots. Therefore,

$$\bar{L}(s_k, j_k, q_k) = \sum_{i=1}^{B_k} \sum_{m} mP\{A(s_k) = C - q_{k,i-1} + m/s_k j_k q_k\}$$

and

$$\bar{L}(s_k, j_k, q_k) = \sum_{i=1}^{B_k} \sum_{l=0}^{C} \sum_{m=0}^{l-C+1} mP\{A(s_k) = C - l + m/s_k j_k q_k\} P\{q_{k,i-1} = l/q_{k,0} = q_k\}.$$

Combining $\bar{L}(s_k, j_k, q_k)$ and $\bar{M}(s_k, j_k, q_k)$ equations obtained above, the ABR cell loss probability, LP, can be expressed as follows.

$$LP = \sum_{s_k=0}^{1} \sum_{j_k=0}^{1} \sum_{q_k=0}^{C} \frac{\Pi(s_k, j_k, q_k)}{B_k + r_i(s_k) B_k T_k} \times \sum_{i=1}^{B_k} \sum_{l=0}^{C} \sum_{m=0}^{l-C+1} mP\{A(s_k) = C - l + m/s_k j_k q_k\} P\{q_{k,i-1} = l/q_{k,0} = q_k\}.$$

4. Numerical results

In this section, some numerical results are presented to illustrate the impact of network and source time scales on the performance of the ABR source away from the network access node. While a large propagation delay (small network time scale) is expected to impact negatively on the performance of the system, the opposite impact is expected from large ABR and VBR time scales.

The performance of the queuing system in terms of cell loss probability for the ABR source is illustrated in Fig. 5. The loss probability is plotted as a function of p_l and the results are derived for a buffer capacity C of 40 and VBR source rates of 0.4 and 0.8 cells/slot. For this plot the $TC(1, T_k)$ transmission policy is used for the ABR source. As the propagation delay decreases (p_l increases), the amount of time that it takes for the ABR source to respond to the VBR source rate changes decreases. As a consequence, the duration of bandwidth mismatch decreases, causing a decrease in the ABR cell loss probability. In addition to the propagation delay, the VBR time scale $1/p_s$ also impacts on the ABR cell loss probability. As the VBR time scale decreases, VBR

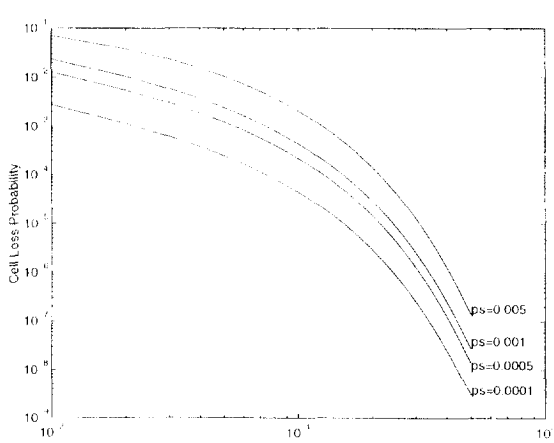

Fig. 5. ABR cell loss probability versus p_l for various p_s.

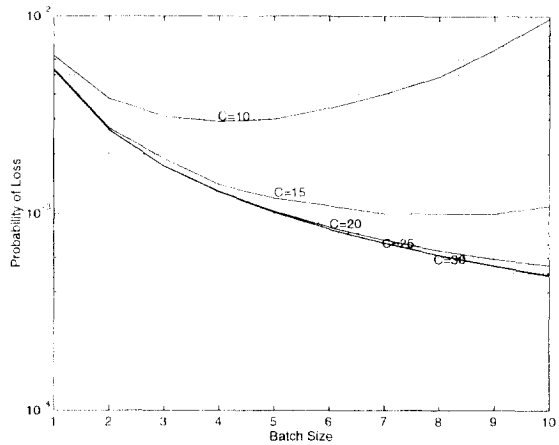

Fig. 6. ABR cell loss probability versus batch size for various values of C.

source rate changes occur more frequently. As a result, more bandwidth mismatch cycles are initiated resulting in more losses. Fig. 5 shows the ABR cell loss probability for $p_s = 0.005$, $p_s = 0.001$, $p_s = 0.0005$, $p_s = 0.0001$ where $p_s = p_s(0) = p_s(1)$. Note that p_s is kept below 0.005 due to the requirement that it should be much less than p_f in order for the assumption of no multiple feedbacks to be reasonably accurate.

In Figs. 6 and 7, the impact of the ABR time scale is illustrated. The ABR cell loss probability is plotted as a function of the batch size B_k for various values of buffer capacities. The VBR source rates are assumed to be equal to 0.4 and 0.8 cells/slot. The average distance between the ABR source and the network access node is assumed to be 10000 subframes (thus $p_f = 10^{-4}$). Note that, the ABR time scale (subframe lengths) is directly proportional to batch sizes, since subframe lengths are equal to $B_k T_k$. For example, for this particular example a batch size of 7 corresponds to subframe lengths of 14 and 42, where the corresponding fundamental subframe lengths are 2 and 6. Because of the single outstanding feedback assumption, p_s is kept much smaller than p_f ($p_s = 10^{-6}$). The ABR loss probability versus the batch size is plotted in Fig. 6 for $C = 10, 15, 20, 25, 30$. It can be clearly observed that for a fixed value of C, the ABR cell loss probability initially decreases as the batch

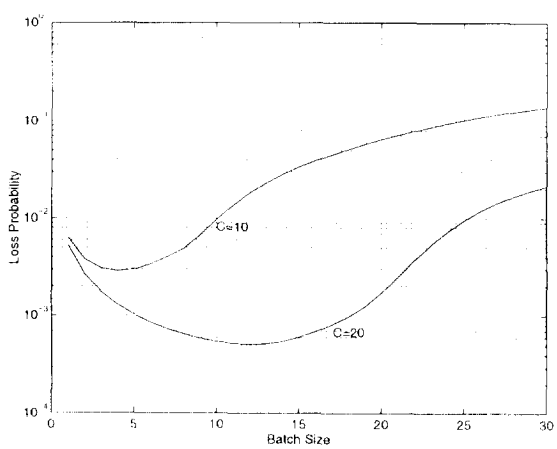

Fig. 7. ABR cell loss probability versus batch size for $C = 10$ and $C = 20$.

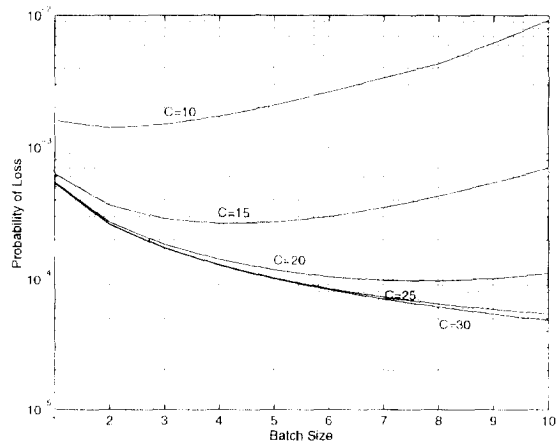

Fig. 8. ABR cell loss probability versus batch size for a distance of 2000 slots.

size (ABR time scale) increases. This behavior is reversed when the batch size exceeds a threshold. Thus, for a given buffer capacity C, there is an optimal batch size (or ABR time scale) that minimizes the induced ABR cell losses. These observations can be made in Fig. 7 where results for a larger range of batch sizes are plotted for $C = 10, 20$.

The reduced ABR losses for batch sizes greater than one may be attributed to the associated increased ABR source time scale. This positive impact prevails as long as the buffer capacity C is large enough to absorb the increased batches. When the batch size exceeds a threshold, it cannot be effectively absorbed by the fixed buffer size, resulting in losses which are not compensated for by the benefits from the increased time scale. The larger the value of C, the larger this threshold is expected to be, as it is clearly observed in Figs. 6 and 7.

The impact of the employed ABR time scale (or batch size) on the system performance is expected to be affected by the propagation delay. Figs. 8 and 9 illustrate the impact of the propagation delay on the performance of the system. Fig. 8 is obtained for an average distance between the ABR source and the network access node equal to 1000 subframes (thus $p_f = 10^{-3}$). Fig. 9 is obtained for an average distance of 100

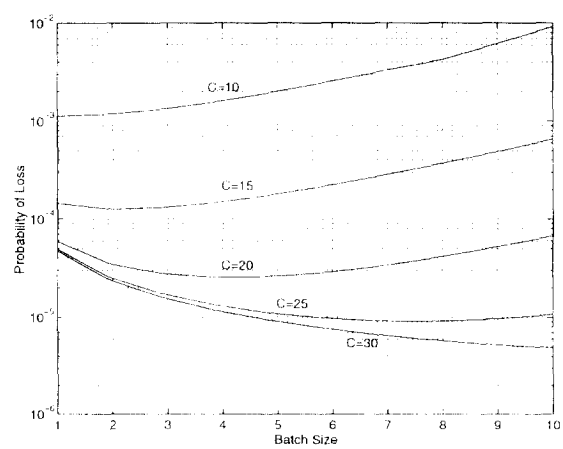

Fig. 9. ABR cell loss probability versus batch size for a distance of 200 slots.

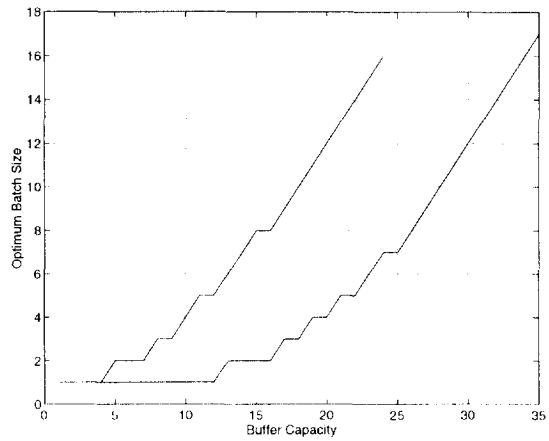

Fig. 10. Optimum batch size versus buffer capacity.

subframes (thus $p_f = 10^{-2}$). As expected, the performance improves under all ABR time scales as the distance decreases, because the amount of bandwidth mismatch is proportional to the distance.

By comparing the plots for $C = 10$ in Figs. 6, 8 and 9 which have been obtained for an average propagation distance of 20000, 2000 and 200 slots, respectively, it may be concluded that the optimal batch size decreases with the propagation distance. For a propagation distance of 200 slots and $C = 10$ the optimal batch size is as low as 1. This trend may be attributed to the decreasing positive impact of a large ABR time scale (batch size) as the propagation delay decreases. This positive impact cannot compensate for the negative impact of a larger batch size, driving the optimal batch size to lower values.

The above can be more clearly observed in Fig. 10 where the optimal batch size against the buffer capacity is plotted for average distances of 20000 and 2000 slots. It can be established that for large propagation distances, the optimal batch size is larger than 1 even for small buffer capacities. Note that the optimal batch size seems to be linearly increasing with the buffer capacity.

In addition to the network and source time scales, the VBR source rates also have considerable effects on the performance. Fig. 11 shows the affects of the VBR source rates on the loss probability. For a fair comparison, the mean VBR arrival rate is kept constant for the cases considered. The VBR source rates for the first case are

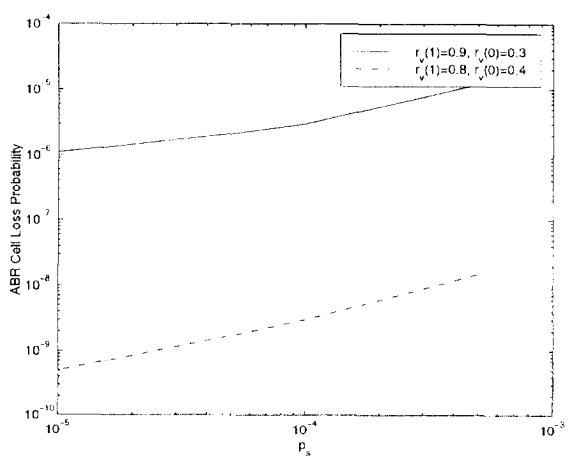

Fig. 11. ABR cell loss probability versus p_s for various VBR arrival rates.

$r_v(1) = 0.9$ and $r_v(0) = 0.3$ cells/slot, while for the second case $r_v(1) = 0.8$ and $r_v(0) = 0.4$ cells/slot. It can be clearly observed that the loss performance improves as the difference between the two rates decreases. For the case with $r_v(0) = 0.3$ and $r_v(1) = 0.9$, the subframe lengths are 2 and 11 slots. These subframe lengths correspond to ABR source rates of 0.5 and 0.091 respectively. Therefore, during a bandwidth mismatch initiated by a VBR source rate change, the total rate on the link can increase up to 1.4 causing potentially high losses. When the VBR source rate drops from 0.9 to 0.3, the total rate in the link decreases to 0.391 causing excessive underutilization. However, when VBR rates are $r_v(0) = 0.4$ and $r_v(1) = 0.8$, the corresponding ABR rates will be 0.5 and 0.167. During a bandwidth mismatch the total rate on the link will be at most 1.3 or at least 0.567. Compared to 1.4 and 0.391, the overutilization and underutilization in this case are decreased. Therefore, a decrease in the ABR cell loss probabilities occurs.

5. Conclusions

In this paper, the impact of network and source time scales on the performance of ABR applications is studied. The network time scale is defined as the transmission time of a cell. The VBR time scale is defined in terms of the rate of change of the VBR source rate. The ABR time scale is defined as the minimum distance between consecutive blocks of consecutive cells generated by the ABR source.

While the impact of the network time scale has been considered in detail in the past, that of other relevant time scales has not been investigated. The main contribution of this paper is the study of the impact of the VBR and ABR time scales on feedback based flow control.

The increased VBR time scale has a positive impact on the ABR loss performance. This is due to the fact that, less frequent VBR rate changes (or bandwidth mismatch cycles) occur when the VBR time scale increases, resulting in reduced ABR cell losses. Increasing the ABR time scale (or the batch size), results in decreased loss probability up to a threshold beyond which the situation is reversed. The optimal batch size – defined to be the one corresponding to this threshold – increases with the buffer capacity, as the capability of absorbing larger batches by the buffer increases with increased buffer space. For large propagation distances the optimal batch size is greater than one, even for small buffer capacities. As the propagation distance decreases, the optimal batch size decreases as well. This may be due to the reduced positive impact of the ABR time scale for decreased propagation delay.

The major conclusion of this work is that in addition to the network time scale, the ABR and VBR time scales may impact substantially a feedback based flow control as well. Thus the impact of *all system time scales* should be considered in order to accurately evaluate the effectiveness of a flow control algorithm. Also, based on this study a new class of transmission policies for the ABR sources is defined which may result in better system efficiency. Thus, departing from the periodic $B_k = 1$ policy, ($B_k = n$ ($n \geq 1$)) policies may be more efficient. Further study will focus on development of a new framework for ABR traffic management based on this new policies.

References

[1] ATM Forum, Traffic Management Specification Version 4.0, ATM Forum/95-0013R10, February 1995.
[2] T. Chen et al., The available bit rate service for data in ATM networks, IEEE Commun. Mag. (May 1996) 56–71.
[3] F. Bonomi, R. Morris, The rate based flow control framework for the available bit rate ATM service, IEEE Network (March/April 1995) 25–39.
[4] J.C. Bolot, A. Shankar, Dynamical behavior of rate based flow control mechanism, ACM Comput. Commun. Rev. (April 1990) 35–49.
[5] S. Liu et al., Fairness in closed loop rate based traffic control schemes, ATM Forum/94-0387, May 1994.
[6] H.T. Kung, R. Morris, Credit based flow control for ATM networks, IEEE Network (March/April 1995) 40–48.

[7] H.T. Kung, K. Chang, Receiver-oriented adaptive buffer allocation in credit-based flow control for ATM networks, INFOCOM'95, 1995, pp. 239–252.
[8] J.F. Ren, J.W. Mark, Design and analysis of a credit based controller for congestion control in B-ISDN/ATM networks, INFOCOM'95, 1995, pp. 40–48.
[9] K.K. Ramakrishnan, P. Newman, Integration of rate based and credit schemes for ATM flow control, IEEE Network (March/April 1995) 49–56.
[10] N. Yin, M.G. Hluchjy, On closed-loop rate control for ATM cell relay networks, INFOCOM'94, Toronto, 1994, pp. 99–108.
[11] R. Beraldi, S. Morano, Selective BECN schemes for congestion control of ABR traffic in ATM LAN, ICC'96, 1996, pp. 503–507.
[12] A. Barnhart, Baseline performance using PRCA rate control, ATM Forum/94-0597, July 1994.
[13] A. Charny et al., Congestion control with explicit rate indications, ICC'95, Seattle, 1995, pp. 1954–1963.
[14] L. Roberts, Enhanced PRCA, ATM Forum/94-0735R1, August 1994.
[15] Y.T. Wang, B. Sengupta, Performance analysis of a feedback congestion control policy under non-negligible propagation delay, ACM SIGCOMM'91, September 1991, pp. 149–157.
[16] M. Abdelaziz, I. Stavrakakis, Study of an adaptive rate control scheme under unequal propagation delays, ICC'95, Seattle, 1995, pp. 1964–1968.
[17] R. Pazhyannur, R. Agrawal, Feedback based flow control in ATM networks with multiple propagation delays, 1996 IEEE, pp. 585–593.
[18] M. Abdelaziz, I. Stavrakakis, Study of the effectiveness of adaptive rate control for slow arrival processes, GLOBECOM'96, London, November 1996, pp. 1102–1106.

Tamer Dağ received the B.S. degree in Electrical Engineering from Middle East Technical University, Ankara, Turkey, in 1994 and the M.S. degree in Electrical Engineering from Northeastern University, Boston, MA, in 1997. He is currently a Ph.D. candidate and a graduate research assistant in the Department of Electrical and Computer Engineering at Northeastern University. His current research interests are in the fields of traffic control in ATM networks and ABR service class.

Ioannis Stavrakakis received the Diploma in Electrical Engineering from the Aristotelian University of Thessaloniki, Greece, in 1983 and the Ph.D. degree in Electrical Engineering from the University of Virginia in 1988. In 1988 he joined the faculty of Computer Science and Electrical Engineering at the University of Vermont as an assistant and then Associate Professor. Since 1994 he has been an Associate Professor of Electrical and Computer Engineering at Northeastern University, Boston. His research interests are in stochastic system modeling, teletraffic analysis, and discrete time queueing theory, with primary focus on the design and performance evaluation of Broadband Integrated Services Digital Networks (B-ISDN). Dr. Stavrakakis is a senior member of IEEE Communications Society, Technical Committee on Computer Communications (TCCC) and a member of IFIP WG6.3. He has organized and chaired sessions, and has been a technical committee member, for numerous conferences sponsored by IEEE, ACM, ITC and IFIP societies such as GLOBECOM, ICC, ICUPC and INFOCOM. He is currently the TCCC conference coordinator and has served as the TCCC representative for ICC'95 conference and as a co-organizer of the 1996 International Teletraffic Congress (ITC) Mini-Seminar, on "Performance Modeling and Design of Wireless/PCS Networks".